Supporting Information

Lee et al. 10.1073/pnas.1414298111

SI Materials and Methods

Side view, real time fluorescent images of AFM compression of live cells was accomplished using a right angle prism positioned to reflect the sideways image down into the inverted optical microscope objective. By placing a 180-μm prism (Precision Optics) within the field of view of the objective, the side view image comes into focus when the objective is moved upward, thereby moving the image plane so that it reflects off the prism and becomes centered on the AFM tip in the plane perpendicular to the microscope slide. The image of the cell and AFM tip appear on the side of the image in the CCD, consistent with the location of the prism. The prism is mounted on a rectangular glass capillary tube to facilitate positioning by a three-axis precision mechanical stage. The AFM tip in this case is a tipless cantilever. The prism has its diagonal face (which faces the AFM tip/cell combination) coated with aluminum for high reflectivity.

SI Results

Kinetic Modeling Suggests Synergy of PIEZO1 and PIEZO2 Channels. To elucidate the mechanism underlying the synergy and to account for the observed characteristics of the channel activity, we fit both Piezo1 and Piezo2 rapidly inactivating currents to a three-state model to calculate its kinetics (Fig. S3). Three states are the minimal model that includes mechanical activation and inactivation. Piezo1 and Piezo2 alone each inactivated to a near-zero plateau, whereas Piezo1/2 together had a pronounced and sustained plateau current. We could not fit the Piezo1/2 data to any three-state model. We then fit the Piezo1/2 data to the sum of currents from noninactivating channels and rapidly inactivating channels and found reasonable agreement (Fig. S3). These data suggest that cotransfection with Piezo1/2 changed the channel kinetics of both kinds of channels, and that the currents did not arise from independent activity of Piezo1 (P1) and Piezo2 (P2).

Attempts to Record Current from Mechanically Stimulated Chondrocytes. We attempted to complement the AFM Ca^{2+} imaging with electrophysiology by stimulating primary articular chondrocytes with micropipettes, as used previously for mechanical stimulation of cells (1, 2). Despite a determined effort, we were not successful in evoking responses, probably because of the small cell size and spherical shape. In addition, excessive stress generated by patch formation or possibly shielding of the channel by the cytoskeleton in the patch could account for this (3). We did not observe unitary ion channel currents in cell-attached mode in response to suction. The latter finding contrasts with our successful implementation in Piezo-transfected N2A cells (see above, see also ref. 1). This may result from the different environments in chondrocytes and N2A cells or reduced functional expression of components of the mechanotransduction apparatus. Moreover, it is well known that the chemical composition and mechanics of patches can be very different from those of the native membrane (4, 5).

Chlorpromazine Does Not Potentiate Low-Dose GsMTx4. To address whether dynasore's effect is based on its amphipathic rather than dynamin GTPase inhibitory properties, we assessed the effect of another amphipathic molecule on "low dose" GsMTx4. Chlorpromazine exerts mechanical effects on lipid membranes (6). It also blocks dopamine receptors in the brain, which are not expressed in cartilage. Chlorpromazine did not affect the potency of 2 μM GsMTx4, suggesting that the dynasore effects were caused by its action as dynamin GTPase inhibitor, and rather not a general property of amphipaths (Fig. S9).

Lack of Off-Target Effects of GsMTx4 on Hypotonicity Evoked Ca^{2+} Influx. With respect to off-target effects of GsMTx4, there was no obvious toxicity or nonspecific inhibition of chondrocyte signaling at 40 μM. This dose of GsMTx4 had no effect on Ca^{2+} influx via TRPV4 when activating the channel using the physiological stimulus, hypotonicity (7) (Fig. S10).

1. Coste B, et al. (2010) Piezo1 and Piezo2 are essential components of distinct mechanically activated cation channels. *Science* 330(6000):55–60.
2. Bae C, Gottlieb PA, Sachs F (2013) Human PIEZO1: Removing inactivation. *Biophys J* 105(4):880–886.
3. Suchyna TM, Markin VS, Sachs F (2009) Biophysics and structure of the patch and the gigaseal. *Biophys J* 97(3):738–747.
4. Ruknudin A, Song MJ, Sachs F (1991) The ultrastructure of patch-clamped membranes: A study using high voltage electron microscopy. *J Cell Biol* 112(1):125–134.
5. Gottlieb PA, Sachs F (2012) Piezo1: Properties of a cation selective mechanical channel. *Channels (Austin)* 6(4):214–219.
6. Chen JY, et al. (2003) Selective amphipathic nature of chlorpromazine binding to plasma membrane bilayers. *Biochim Biophys Acta* 1616(1):95–105.
7. Phan MN, et al. (2009) Functional characterization of TRPV4 as an osmotically sensitive ion channel in porcine articular chondrocytes. *Arthritis Rheum* 60(10):3028–3037.

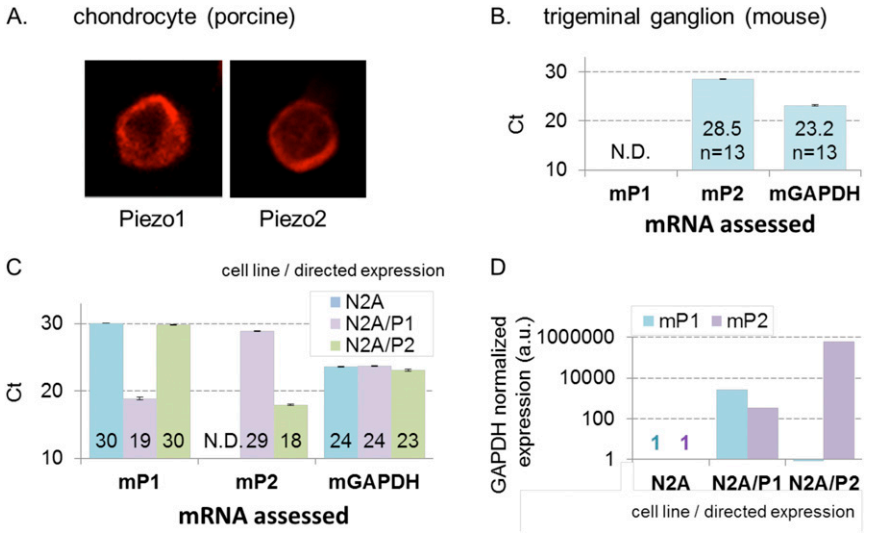

Fig. S1. Supplementary Piezo1/2 gene expression data and directed expression in N2A cells. (*A*) Positive Piezo1 and Piezo2 staining of isolated porcine chondrocytes, supplementing main Fig. 1*E*. (*B*) Ct values of mouse trigeminal ganglion (TG) RT-qPCR for Piezo1/2. Note that Piezo2 is expressed at approximately similarly robust levels in TG as it is in chondrocytes, supplementing main Fig. 1 *C* and *D*. (*C*) RT-qPCR N2A cells transfected with control, Piezo1, or Piezo2. N.D., not detectable. (*D*) Results from *C* normalized for control. Note that Piezo1 expression also evokes Piezo2 mRNA, but not the other way around. (*A*–*C*) Primer sequences of mPiezo1 and mPiezo2 are adopted from ref. 1.

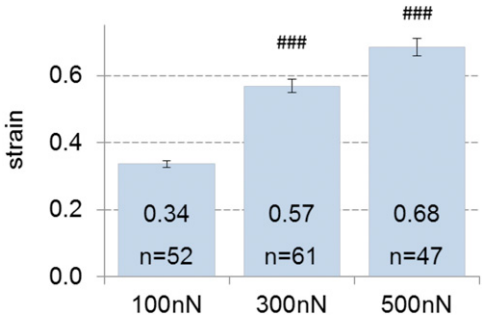

Fig. S2. Strain–force relationship of N2A cells. The nominal strain (final cell height divided by original cell height) was determined as a function of applied force. $^{###}P < 0.0005$ significantly different from all other forces (ANOVA, LSD post hoc).

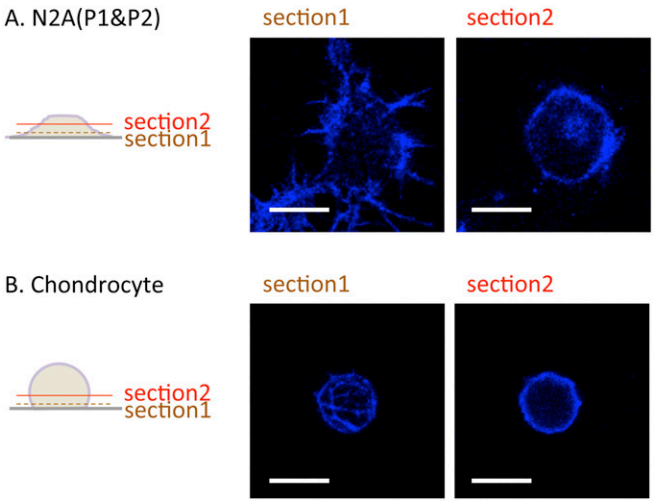

Fig. S3. Similar cytoarchitecture of the actin cytoskeleton in N2A cells coexpressing Piezo1/Piezo2 and articular chondrocytes. Representative confocal micrographs of an N2A cell (permanent cell line) (*A*) and a primary articular chondrocyte (*B*), note the β-actin cytoskeleton labeled with blue fluorescent phalloidin. (Scale bar, 10 μm.) Left schematic illustrates the depth of the cross-section. Section 1 indicates that N2A(P1/P2) is characterized by a spread-out shape, whereas primary chondrocytes appear rounded. Note also that Piezo1 cDNA transfected into N2A cells was the version with an external bungarotoxin-binding site (a fully functional Piezo1 isoform).

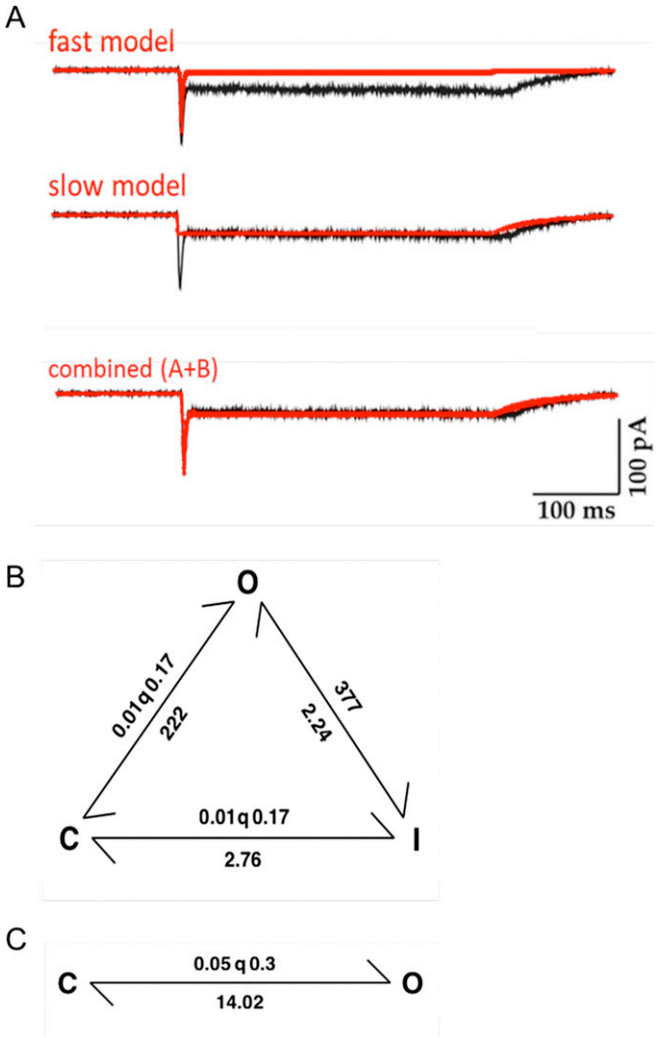

Fig. S4. Modeling of mechanically evoked currents recorded from a patch of N2A cells overexpressing Piezo1/2. The question was whether the standard three state models for Piezo1 or -2 could fit the data from P1/P2 coexpression. Can the data be explained by the overlap of currents from two independent channels? The fitting used www.qub.buffalo.edu MAC software. (*A*) Optimal fit of the standard closed-open-inactivated loop model (1). (*B*) Emphasizing the transient phase of P1/P2 data. The fit is poor and no manipulations of the rates or the mechanical sensitivities would improve the fit. The main problem was getting a steady plateau. The next simplest model was to combine the model in *B* with an independent two-state noninactivating channel (2) (*C*, slow model in *A*, *Middle*). The sum of the two models provided a good fit and is equivalent to a five-state model constrained by independence. Rate constants are in the units of s^{-1} and the number following the symbol *q* is the stress sensitivity of that rate in $mmHg^{-1}$. The most distinct difference between P1, P2, and P1/P2 is that the latter has a noninactivating plateau not present in the others.

1. Bae C, Gottlieb PA, Sachs F (2013) Human PIEZO1: Removing inactivation. *Biophys J* 105(4):880–886.
2. Bae C, Gnanasambandam R, Nicolai C, Sachs F, Gottlieb PA (2013) Xerocytosis is caused by mutations that alter the kinetics of the mechanosensitive channel PIEZO1. *Proc Natl Acad Sci USA* 110(12):E1162–E1168.

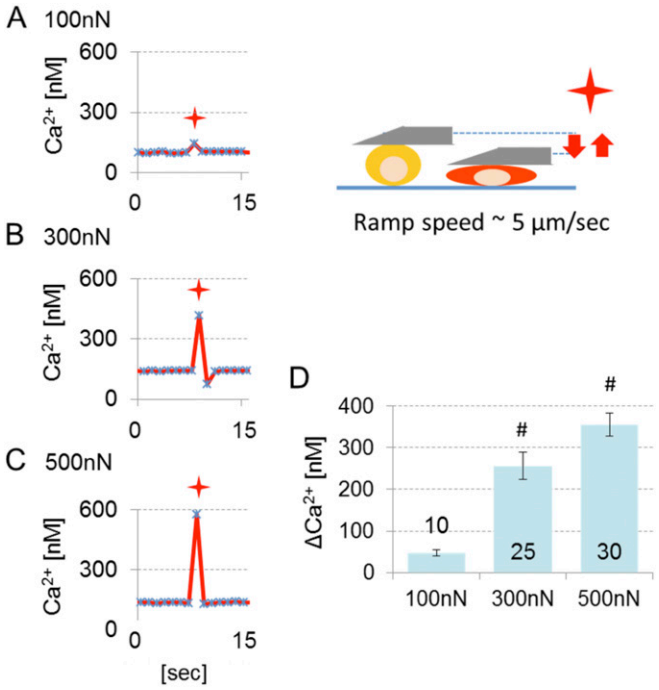

Fig. S5. Increased mechanical loading induced higher Ca^{2+} transients in chondrocytes. Primary chondrocytes were compressed by AFM probes with trigger forces of 100 nN, 300 nN and 500 nN in ramp mode (*Top Right*). (*A*–*C*) Representative resulting Ca^{2+} transients at each force are shown. (*D*) Higher mechanical loading induced chondrocytes to influx more [Ca^{2+}]. $^{\#}P < 0.05$, significantly different from all other forces (ANOVA, LSD post hoc).

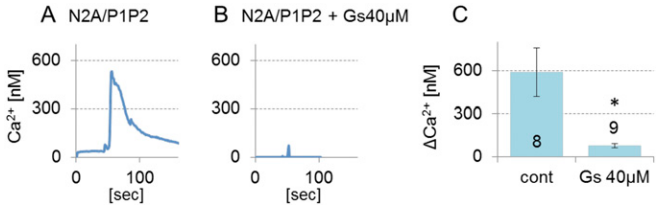

Fig. S6. GsMTx4 reduces compression-induced Ca^{2+} transients in N2A cells overexpressing Piezo1 and Piezo2. Compression by AFM with 400 nN at 1 µm/s. (*A*) Piezo1/2-directed expression, vehicle control, note the robust and prolonged Ca^{2+} transient. (*B*) Ca^{2+} transients are eliminated upon exposure to 40 µM GsMTx4; also note the greatly reduced base-line Ca^{2+}. (*C*) Ca^{2+} transients were significantly different from control. Numbers in or above bars denote assessed number of cells. $^{*}P = 0.006$, unpaired *t* test.

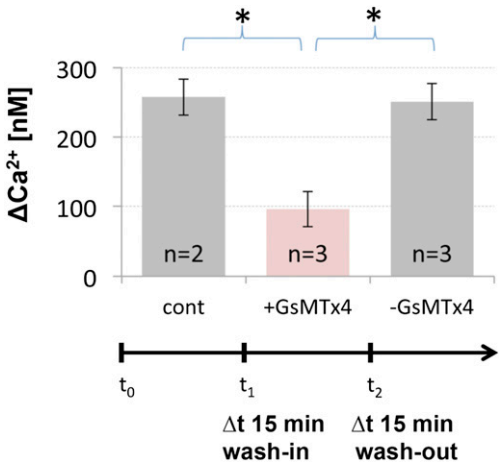

Fig. S7. Washout of GsMTx4 restores the AFM-compression Ca^{2+} response in primary chondrocytes.

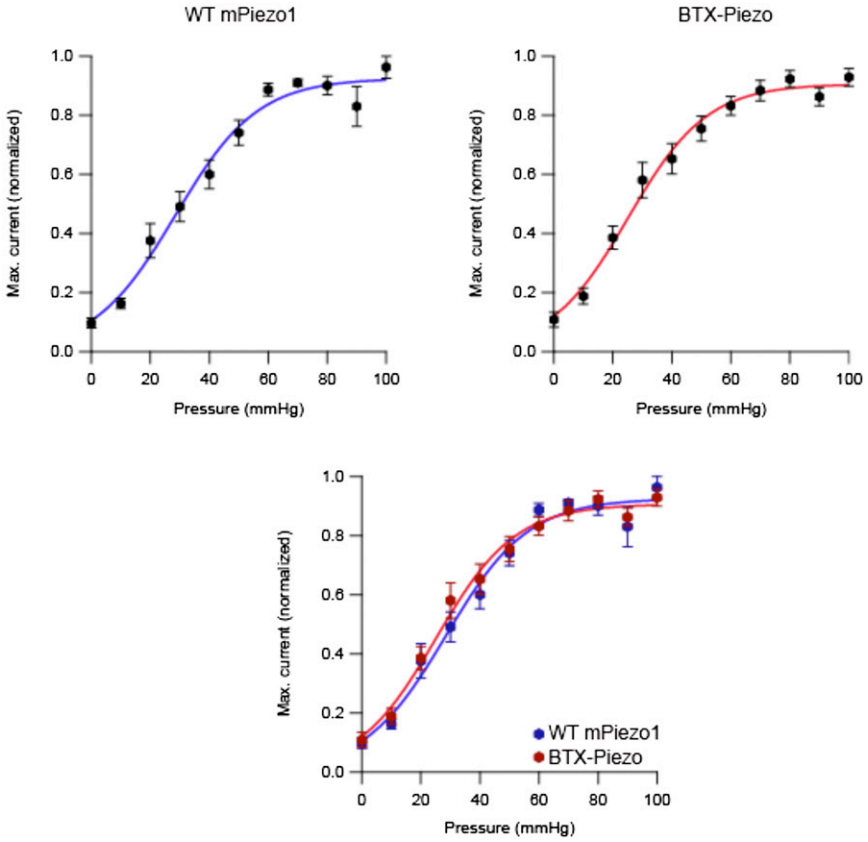

Fig. S8. Conserved functionality of Piezo1 channels engineered to bind bungarotoxin extracellularly. Normalized current–pressure relationship of stretch-activated currents at −80 mV fitted with a Boltzmann equation for WT mPiezo1 ($n = 14$, $P_{50} = 32.9 \pm 3.4$ mmHg) and BTX-Piezo ($n = 14$, $P_{50} = 27.8 \pm 2.7$ mmHg). Pressure of half maximal activation (P_{50}) is the average of P_{50} values determined for individual cells. Bars represent mean ± SEM.

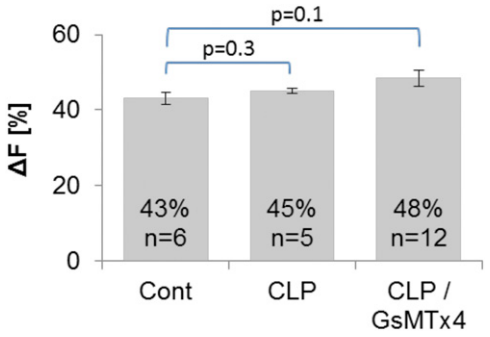

Fig. S9. Effect of chlorpromazine (CLP) and "low-dose" GsMTx4 on the Ca^{2+} response of chondrocytes evoked by AFM-mediated compression. CLP 100 μg/mL with or without GsMTx4 (2 μM) did not suppress the compression-induced Ca^{2+} responses. $\Delta F\,[\%] = (F_{max} - F_{basal})/F_{basal} \times 100$ (using fluo-4 Ca^{2+} sensitive dye); P values of unpaired t test.

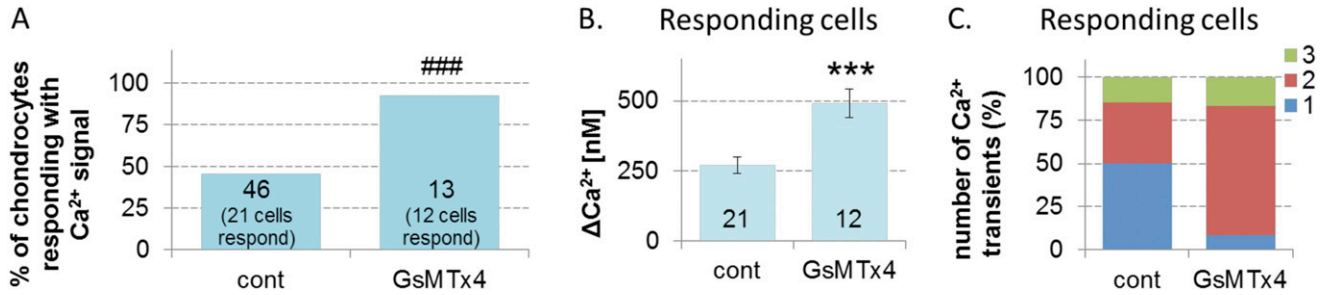

Fig. S10. Effect of GsMTx4 on the hypotonicity-evoked Ca^{2+} response of chondrocytes. Note that GsMTx4 (40 μM) did not suppress but rather induced a more pronounced Ca^{2+} response of chondrocytes in response to 253 mOsm hypotonicity. (*A*) For all cells, percent responding cells; (*B*) only for responder cells; and (*C*) detailed analysis in terms of repeat transients (oscillating Ca^{2+} transient). $^{###}P < 0.0005$, χ^2 test; $^{***}P < 0.0005$, unpaired *t* test.

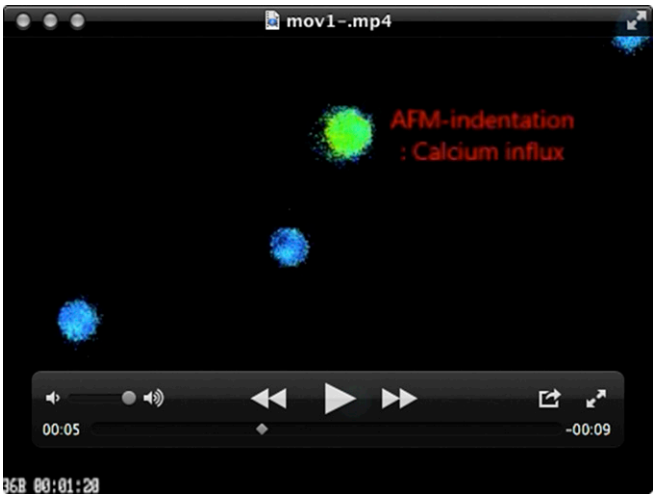

Movie S1. AFM-mediated compression of chondrocytes: Ca^{2+} imaging.

Movie S1

Movie S2. AFM-mediated compression of chondrocytes: lateral view.

Movie S2